

Cavity and HOM Coupler Design for CEPC*

ZHENG Hong-Juan (郑洪娟)¹, GAO Jie (高杰)¹, LIU Zhen-Chao (刘振超)¹

¹ (Key Laboratory of Particle Acceleration Physics and Technology, Institute of High Energy Physics, CAS, Beijing 100049, China)

Abstract: In this paper we will show a cavity and higher order mode (HOM) coupler designing scheme for the Circular Electron-Positron Collider (CEPC) main ring. The cavity radio frequency (RF) design parameters are showed in this paper. The HOM power is calculated based on the beam parameters in the Preliminary Conceptual Design Report (Pre-CDR). The damping results of the higher order modes (HOMs) and same order modes (SOMs) show that they are reached the damping requirements for beam stability.

Keywords: CEPC, 650 MHz 5-cell superconducting cavity, HOM coupler, higher order modes, Q_e , damping requirements

PACS: 29.20.Ej

1 Introduction

With the discovery of Higgs boson on LHC in 2012, the world's high energy physics (HEP) community is interested in future large circular colliders to study the Higgs boson. Because the Higgs mass is low (126 GeV), a circular e^+e^- collider can serve as a Higgs factory. The Institute of High Energy Physics (IHEP) in Beijing, in collaboration with a number of other institutes, launched a study of 50-100 km ring collider [1]. It will serve as an e^+e^- collider for the Higgs factory with the name of Circular Electron-Positron Collider (CEPC). A Preliminary Conceptual Design Report (Pre-CDR) was published on March, 2015 [2].

The circumference of the main ring is 54.7 km with 2 beams in one ring. The synchrotron radiation power for one beam is 51.7 MW. Table 1 shows the main parameters of the CEPC main ring [2]. The radio frequency (RF) system accelerates the electron and positron beams, compensates the synchrotron radiation loss and provide sufficient RF voltage for energy acceptance and the required bunch length in the collider. Superconducting Radio Frequency (SRF) cavities are used because they have much higher continuous wave (CW) gradient and energy efficiency as well as large beam aperture compared to normal conducting cavities. CEPC will use 384 five-cell 650 MHz cavities for the main ring. The cavity design and HOM power analysis are shown in this paper.

2 Cavity design

The geometry of the superconducting cavity is shown in Fig. 1. The meaning and the effects of the cavity parameters are summarized in the following:

- 1) R_{iris} is the radius of the iris. Fig. 2 (a) shows that large R_{iris} is good for the cell-to-cell coupling. However, large R_{iris} leads to large E_p/E_{acc} and H_p/E_{acc} value. Large R_{iris} value also decreases the impedance of the

fundamental mode.

- 2) D is the radius of the equator. It is used for the frequency tuning.

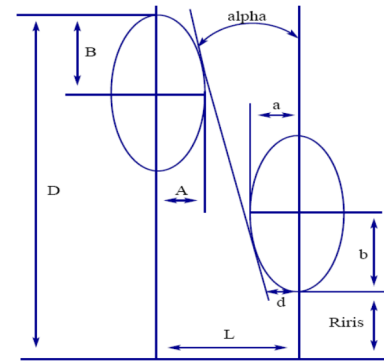


Fig. 1. The definition of cell shape parameters.

- 3) L is the half length of the cavity cell. It is determined by the fundamental frequency and the cavity geometry beta.
- 4) The equator ellipse ration (B/A) is ruled by the mechanical considerations.
- 5) The iris ellipse ration (b/a) is determined by the local optimization of the peak electric field. Fig. 2 (b) shows that the iris ellipse ration is sensitive to E_p/E_{acc} and cell-to-cell coupling. It has a little effect on H_p/E_{acc} and R/Q .
- 6) α is the side wall inclination. Fig. 2 (c) shows that the angle has a little effect on R/Q . Small α decreases the H_p/E_{acc} value while increases the cell-to-cell coupling. However, small α increases the E_p/E_{acc} value. The higher angle is better for the cavity chemistry and cleaning procedures.
- 7) d is the wall distance parameter. Fig. 2 (d) shows when d increases, E_p/E_{acc} will decrease while H_p/E_{acc} will increase. The parameter d is used to balance the E_p/E_{acc} and H_p/E_{acc} value. However, smaller d also increases the cell-to-cell coupling.

* Supported by National Natural Science Foundation of China (11175192).

1) E-mail: zhenghj@ihep.ac.cn

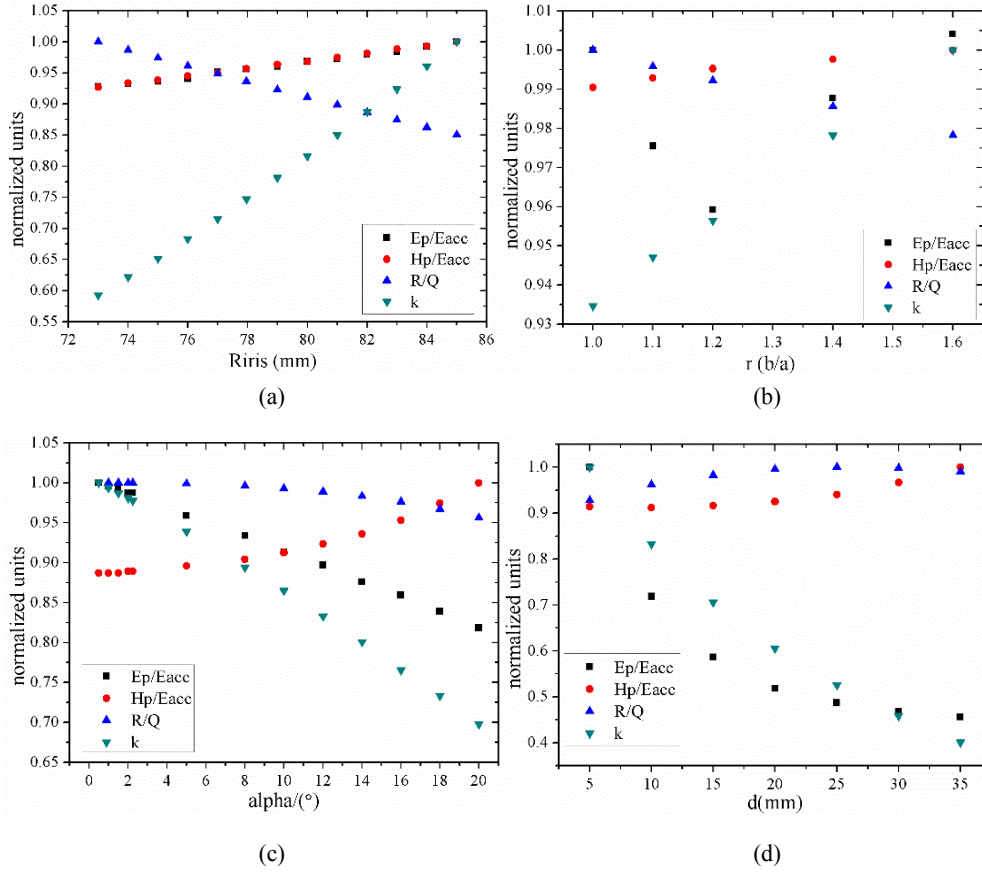


Fig. 2. Electromagnetic parameters as a function of R_{iris} , b/a , α , d .

Table 1. Main parameters for CEPC main ring.

Parameter	Unit	Value	Parameter	Unit	Value
Beam energy	GeV	120	Circumference	m	54752
Number of IP		2	SR loss/turn	GeV	3.11
Bunch number/beam		50	Bunch population		3.79E+11
Synchrotron radiation (SR)	MW	51.7	Beam current	mA	16.6
power/beam					
Bending radius	m	6094	Momentum compaction factor		3.36E-5
Revolution period	s	1.83E-4	Revolution frequency	Hz	5475.46
Emittance (x/y)	nm	6.12/0.018	β_{IP} (x/y)	mm	800/1.2
Transverse size (x/y)	μm	69.97/0.15	$\xi_{x,y}/IP$		0.118/0.083
Bunch length SR	mm	2.14	Bunch length total	mm	2.65
Lifetime due to Beamstrahlung	min	47	Lifetime due to radiation Bhabha scattering	min	51
RF voltage	GV	6.87	RF frequency	MHz	650
Harmonic number		118800	Synchrotron oscillation tune		0.18
Energy acceptance RF	%	5.99	Damping partition number		2
Energy spread SR	%	0.132	Energy spread BS	%	0.096
Energy spread total	%	0.163	During the collision		0.23
Transverse damping time	turns	78	Longitudinal damping time	turns	39
Hourglass factor	Fh	0.68	Luminosity/IP	$\text{cm}^{-2}\text{s}^{-1}$	2.04E+34

We use the code Buildcavity [3] and Superfish [4] to do the parameter san analysis. The optimized parameters of the cavity based on the analysis above are shown in Table 2. The cell shape parameters are shown in Table 3.

The asymmetric end cell design is better to extract the HOMs. The cut-off frequency of the waveguide modes for the beam pipe are 1.355 GHz (TM01) and 1.04 GHz (TE11).

Table 2. The 650 MHz superconducting cavity parameters.

Parameter	Value
Operating frequency/ MHz	650
No. of cells	5
Cavity effective length/ mm	1147
Cavity iris diameter/ mm	156
Beam tube diameter/ mm	170
Cell-to-cell coupling	3%
$R/Q/ \Omega$	514
Geometry factor/ Ω	268
E_p/E_{acc}	2.4
$(H_p/E_{acc}) / (mT/(MV/m))$	4.23
Acceptance gradient/ MV/m	20
Acceptance Q_0	4E10

Table 3. The 650 MHz superconducting cavity cell shape parameters.

Parameters	Mid-cell	Left end cup	Right end cup
L/ mm	115	114	113
R_{iris}/ mm	78	84.5	84.5
A/ mm	94.4	92.1	91
B/ mm	94.4	92.1	91
a/ mm	20	13.8	13.7
b/ mm	22.1	21.1	20.3
D/ mm	206.6	206.6	206.6
$\alpha_{\text{phal}} (^\circ)$	2.24	16.7	16.4

3 HOM power

The bunch length of the main ring is 2.65 mm with a bunch population of 3.78E11. The total longitudinal loss factor of the cavity can be calculated by the program ABCI [5]. The loss factor of the HOMs and the total HOM power can be get by

$$k_0 = \frac{\omega_0}{4} \cdot \frac{R}{Q} \cdot e^{-a_0^2 (\sigma_z/c)^2} \quad (1)$$

k_0 is the loss factor of the fundamental mode. ω_0 is the frequency of the fundamental mode. R/Q is the ratio of the transverse shunt impedance to its quality factor for the fundamental mode. σ_z is the bunch length. c is the speed of light.

$$k_{\text{HOM}} = k_t - k_0 \quad (2)$$

k_{HOM} is the loss factor of the HOMs. k_t is the total loss factor from ABCI.

$$P_{\text{HOM}} = 2k_{\text{HOM}} \cdot Q_b \cdot I_0 \quad (3)$$

P_{HOM} is the HOM power. Q_b is the bunch charge. I_0 is the beam current. 2 means two beam in one ring. According to the simulation results, the loss factor of the HOMs is 1.8 V/pC. The HOM power for each cavity is 3.6 kW. Below the cut-off frequency ($f=1.355$ GHz) of the beam pipe, all power should

be extracted by the HOM coupler. Fig. 3 shows the distribution of power from the cavity HOM properties.

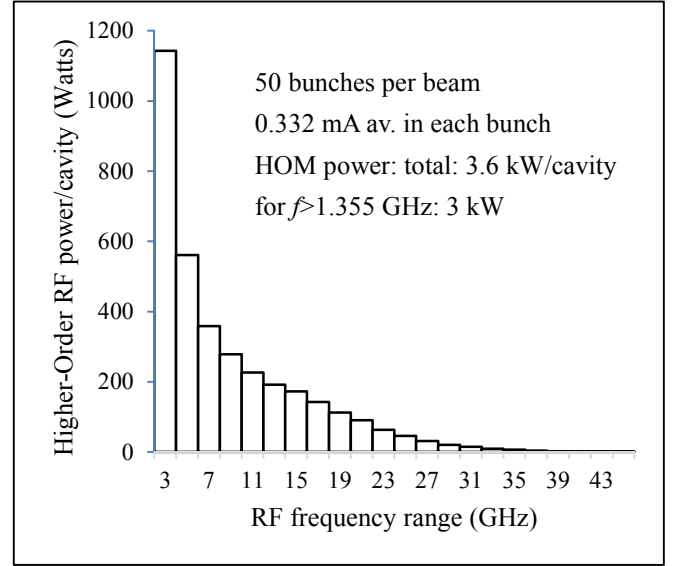


Fig. 3. Frequency distribution of HOM power.

4 SOMs and HOMs damping

4.1 SOMs damping

There are other four passband modes of the operating mode which are called the Same Order Modes (SOMs). Since the SOMs are close in frequency to the operating mode, they can't be damped in the same way as the HOMs. These modes may drive instabilities or extract significant RF power from the beam. We consider to use the input coupler as the SOM coupler. The external quality factor (Q_e) of the input coupler for the fundamental mode is 2.2E6. Both 2-D model and 3-D model are used to calculate the Q_e of SOMs. The results are shown in Table 4.

In a storage ring, the beam instabilities in both the longitudinal and the transverse directions caused by a RF system are mainly from the cavities. To keep the beam stable, the radiation damping time should be less than the rise time of the multi-bunch instability. The threshold for the longitudinal impedance is given by [6]

$$R_L^{\text{thresh}} = \frac{2(E_0/e)v_s}{N_c f_L I_0 \alpha_p \tau_z} \quad (4)$$

E_0 is the beam energy. e is the electronic charge. v_s is the synchrotron oscillation tune. N_c is the total number of cavity. f_L is the mode frequency. α_p is the momentum compaction factor. τ_z is the longitudinal damping time. Bringing the beam parameters from Table 1 into this equation, the longitudinal impedance threshold for different modes can be get.

The threshold of the external quality factor of the mode is given by

$$Q_{\text{limit}} = \frac{R_L^{\text{thresh}}}{R/Q} \quad (5)$$

According to the equation (4) and (5), the Q_{limit} results are also shown in Table 4.

If we consider the worst case, all the modes are on resonance ($\Delta\omega T_b=0$, $T_b \ll T_d$) [7]. The power dissipated by the beam is

$$P_{b,n} = \frac{R_a I_0^2}{1 + \beta} \quad (6)$$

$$\beta = \frac{Q_0}{Q_c} \quad (7)$$

R_a is the shunt impedance of the mode. β is the coupling factor. Q_0 is the unloaded quality factor. T_b is the bunch spacing time. T_d is the decay time of the mode.

If we consider the real cavity passband modes frequencies and the bunch time spacing of the collider ($\Delta\omega T_b \neq 0$), the power dissipated by the beam is

$$\omega_n = \omega + \Delta\omega \quad (8)$$

$$\omega = \frac{2\pi h}{T_b} \quad (9)$$

$$F_r = \frac{1 - \exp(-2\frac{T_b}{T_d})}{2[1 - 2\exp(-\frac{T_b}{T_d})\cos(\Delta\omega T_b) + \exp(-2\frac{T_b}{T_d})]} \quad (10)$$

$$T_d = \frac{2Q_L}{\omega_n} = \frac{2Q_0}{\omega_n(1 + \beta)} \quad (11)$$

$$P_{b,n} = \frac{R_a I_0^2 T_b F_r}{1 + \beta T_d} \quad (12)$$

ω_n is the frequency of the SOM. The integer h is the harmonic number of the beam and ω is the frequency that governs the bunch spacing. Q_L is the loaded quality factor.

The power dissipated by the beam can be get by the analysis above. The results are shown in Table 4. $P_{\text{SOM-res}}$ stands for the worst case and P_{SOM} stands for the general case. The analysis results show that the total SOM power is quite small when we consider the real cavity passband modes frequencies and the bunch time spacing of the collider. Even assuming resonant excitation, the total SOM power is about 1 kW and with the input coupler damping, the power dissipated on the cavity wall is negligible (~ 0.1 W). In other words, the damping for the SOMs by the input coupler are very efficient.

4.2 HOMs damping

Higher order modes excited by the intense beam bunches must be damped to avoid additional cryogenic loss and multi-bunch instabilities. This is accomplished by extracting the stored energy via HOM couplers mounted on both sides of the cavity beam pipe and the HOM absorbers outside the cryomodule.

Table 4. SOMs damping of the 650 MHz 5-cell cavity by the input coupler.

Mode	f (MHz)	R/Q (Ω)	Q_{limit}	Q_c	P_{SOM} (W)	$P_{\text{SOM-res}}$ (W)
$\pi/5$	632.322	0.02	4.5E+9	1.2E+07	1.3E-5	268.9
$2\pi/5$	637.099	0.00017	5.4E+11	3.3E+06	8.7E-7	0.6
$3\pi/5$	643.139	0.341	2.6E+8	1.7E+06	9.31E-3	638.9
$4\pi/5$	648.146	0.078	1.1E+9	1.2E+06	2.92E-4	105.8

There are three major varieties of HOM couplers mainly used: waveguide, coaxial and beam tube. The coaxial HOM coupler is prevalent on several SRF cavity designs, such as XFEL, ILC, and SNS. There have challenges revealed with loop couplers in operating machines, such as with antenna overheating, multipactor, and mis-tuning due to fabrication variations. Beam tube couplers use large diameter beam pipes so as to reduce the R/Q values of the HOMs, as well as to propagate the HOMs freely out of the cavity to high power located at room temperature. This type of couplers will decrease the accelerating efficiency. They are mainly used for high current applications, such as KEK-B and CESR-III. The waveguide coupler has the benefit of transporting the HOM power to external room temperature loads. The cut-off is a natural rejection filter for the fundamental mode. It has the high power handling capability. The structure of waveguide

coupler is simple. The waveguide coupler has been used in several facilities, such as PEP-II, CEBAF and JLab high current cryomodule design [8].

The waveguide couplers are chose for HOMs damping. The high-pass filtering characteristics of waveguide is used to make the operating frequency of cavity under the cut-off frequency of waveguide. The higher order modes can propagate from the waveguide. We choose the cut-off frequency a little lower than the first higher order mode as the cut-off frequency of the waveguide. There are five waveguide HOM couplers and one coaxial main coupler spaced quite symmetrically to minimize transverse kick to the beam. The angular arrangement takes care of all mode polarizations. The five cell cavity with waveguide couplers is shown in Fig. 4.

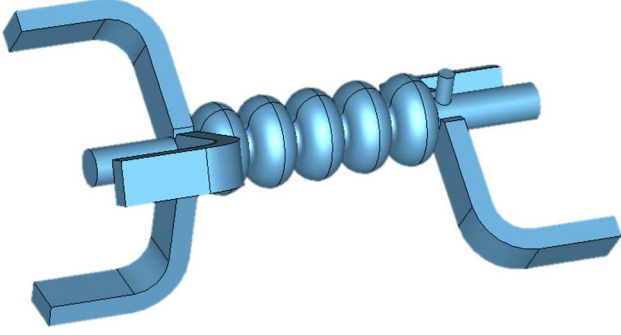


Fig. 4. 5 cell cavity with waveguide HOM couplers.

The higher order modes of the accelerating cavities will lead to the coupled bunch instability. The threshold for the longitudinal impedance is given by equation (4). The transverse coupled bunch instability is mainly caused by the dipole modes in the cavity. The threshold for the transverse impedance can be expressed as

$$R_T^{\text{thresh}} = \frac{2(E_0/e)}{N_c f_{\text{rev}} I_0 \beta_{x,y} \tau_{x,y}} \quad (13)$$

where f_{rev} is the revolution frequency, $\beta_{x,y}$ is the beta function in the RF cavity region, and $\tau_{x,y}$ is the transverse damping time.

The HOMs are calculated up to 2 GHz. The simulation results compared with the impedance threshold are shown in Fig. 5 and Fig. 6. Fig. 5 shows the damping results for the monopole modes. As can be seen from the results, the damping for all the monopole modes are under the longitudinal impedance threshold. The Q_e for fundamental mode is $4E11$. The Q_e for most of monopole modes is below 10^3 while only a few of them is above 10^5 . The HOM power loss on the cavity is only a few milliwatts if the Q_0 of the monopole mode is 10^{10} . Fig. 6 shows the damping results for the dipole modes. Most of the dipole modes damping results are under the transverse impedance threshold. However, we didn't take into account the spread in the resonance frequencies of different cavities. If the frequency spread is 0.5 MHz, the impedance threshold can increase 1~2 orders of magnitude [9]. So, this design can meet the requirements for beam stability.

5 HOM check

Two separate eigenmode simulations for just a single cell, with periodic boundary conditions (PBC) [10], were computed. One can control the phase shift from one cell to the other when using the PBC. In the end, 34 modes up to 1.8 GHz were calculated. One can get the resonant frequency of the fundamental 0-mode f_0 (0° phase shift at PBC) and the π -mode f_π (180° phase shift at PBC). The same rules apply to the higher order modes. To calculate the cell-to-cell coupling factor one needs only f_0 and f_π

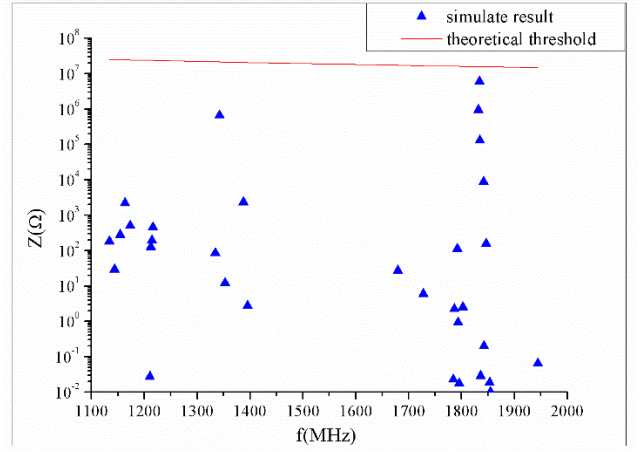


Fig. 5. Monopole modes damping results compared with impedance threshold.

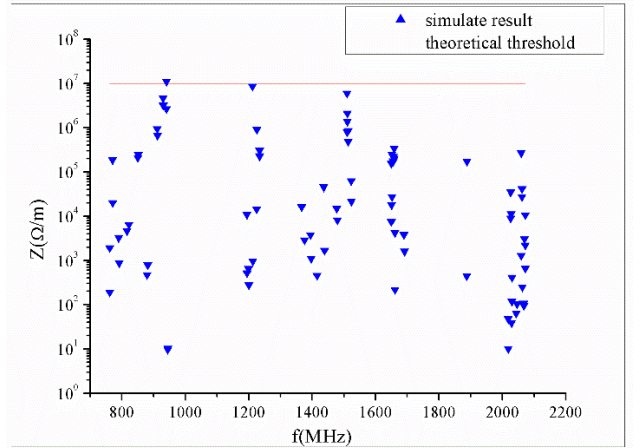


Fig. 6. Dipole modes damping results compared with impedance threshold.

$$k_{cc} = 2 \cdot \frac{f_\pi - f_0}{f_\pi + f_0} \quad (14)$$

The factor k_{cc} specifies the passband width and smaller k_{cc} gives narrower passband. For small ($|k_{cc}| \leq 0.01$) values, there is a danger that if the given mode is excited by the beam, e.g., somewhere in the middle of the cavity, it will propagate out and decay very slowly. Thus the factor k_{cc} give us a preliminary knowledge of which modes can be dangerous or trapped. The results of the eigenmode analysis are listed in Table 5, including the f_0 and f_π of all the modes, mode type, cell-to-cell coupling, and mode impedance. There are two modes with small k_{cc} values, one of which is TE M3 mode. And the other one is TM D5 mode. After the field pattern analysis, the TE M3 mode is TE011 mode and the TM D5 mode is TM120 mode. There is no longitudinal electric field on axis for monopole mode TE012. The impedance for the dipole mode TM120 is also under the impedance threshold ($10^7 \Omega/m$). Although the cell-to-cell coupling factors of the two modes are small, they are no dangerous.

6 Conclusion

In this paper, we give a reasonable cavity and HOM coupler design scheme for the CEPC main ring. The cavity

parameters are given in the paper. The frequency distribution of the HOM power shows that the total HOM power for each cavity is 3.6 kW. After the waveguide HOM coupler introduced to the cavity, all the HOMs are under the

impedance threshold. The SOMs are also damped successfully by the input coupler. All of the analysis results show that the damping scheme are successful.

Table 5. Eigenmode analysis results.

Phase advance 0°			Phase advance 180°			type	k_{cc}
mode	f (MHz)	$Z=(R/Q)*Q_e$	mode	f (MHz)	$Z=(R/Q)*Q_e$		
1	0.630	1.21E+11	1	0.650	9.15E+13	TM M1	0.0303
2,3	0.759	1.91E+3	4,5	0.887	2.46E+5	TE D1	0.1551
4,5	0.946	1.03E+1	2,3	0.877	8.00E+2	TM D2	-0.075
8	1.182	1.79E+2	8	1.130	5.02E+2	TM M2	-0.0466
9	1.213	2.7E-2	11	1.218	1.43E-3	TE M3	0.0045
10,11	1.238	1.63E+4	16,17	1.361	1.67E+3	TM D3	0.0948
14	1.331	8.48E+1	18	1.400	2.76	TM M4	0.0506
17,18	1.479	5.93E+6	19,20	1.509	2.15E+4	TE D4	0.0202
27,28	1.652	1.56E+5	29,30	1.661	4.26E+3	TM D5	0.0057
35	1.802	-----	31	1.665	2.69E+1	TM M4	-0.0791

References

- 1 Wang Dou, Gao Jie, Xiao Ming et al. Chinese Physics C, 2013 37 (9): 097003-097003
- 2 The CEPC-SPPC Study Group. CEPC-SPPC Preliminary Conceptual Design Report, Volume II. IHEP-CEPC-DR-2015-01, IHEP-AC-2015-01, March 2015.
- 3 <http://www.srf.mil.infn.it/Members/pierini>
- 4 http://laacg.lanl.gov/laacg/services/download_sf.shtml
- 5 <http://abci.kek.jp/abci.htm>
- 6 Sun An, Joo Young-Do, Kang Heung-Sik. Journal of the Korean Physical Society, Vol. 56, No. 6, June 2010. 2024:2028
- 7 Hasan Padamsee. RF Superconductivity for Accelerators. WILEY-VCH Verlag GmbH & Co. KGaA, 2008. 10:19, 335:339
- 8 Marhause F. ERL Workshop, June 8, 2009.
- 9 Wang Na, Zheng Hong-juan, Wang Yi-wei et al. HF2014, October 11, 2014.
- 10 Galek T. et al. ICAP2012, August 19, 2012. 152:154